Environmental Science and Pollution Research (2024) 31:42342–42356
https://doi.org/10.1007/s11356-024-33932-4

RESEARCH ARTICLE

Study on harmless treatment of electrolytic manganese residue by low temperature thermochemical method

Zhihan Xie[1,2] · Rongjin Liu[1,2,3,4] · Fuhua Lu[1,2] · Daiyan Jing[2] · Yanrong Zhao[1,2,3,4] · Jianbo Liang[1,2] · Wanyu Huang[1,2] · Yuhang Liu[1,2]

Received: 27 December 2023 / Accepted: 3 June 2024 / Published online: 13 June 2024

Abstract

The Electrolytic Manganese Residue (EMR) is a by-product of the electrolytic manganese metal (EMM) industry, containing high concentrations of potential pollutants such as NH_4^+-N and soluble Mn^{2+}. These components pose a serious threat to the ecological environment. To explore accurate, efficient, and harmless treatment methods for EMR, this study proposes a low-temperature thermochemical approach. The orthogonal experiment design investigates the effects of reaction temperature, reaction time, quicklime (CaO), sodium carbonate (Na_2CO_3), sodium phosphate (Na_3PO_4) (Reviewer #3), and water consumption on manganese solidified and ammonia removal from EMR. The results indicate that optimal conditions are a reaction temperature of 60 ℃ (Reviewer #3) and a reaction time of 10 min. CaO precipitates Mn^{2+} as manganese hydroxide ($Mn(OH)_2$) (Reviewer #3), achieving effective manganese solidified and ammonia removal. The addition of Na_2CO_3 causes Mn^{2+} to form manganesecarbonate ($MnCO_3$) (Reviewer #3)precipitate, while Na_3PO_4 makes Mn^{2+} form Manganese phosphate trihydrate ($Mn_3(PO_4)_2{\cdot}3H_2O$) (Reviewer #3). Increased water consumption enhances the interaction adequacy between ions. Under optimal conditions (CaO 10%, Na_2CO_3 1%, Na_3PO_4 0.5%, and 80% water consumption), the removal rate of ammonium ions reaches 98.5%, and the solidification rate of soluble Mn^{2+} is 99.9%. The order of influence on ammonium ion removal is CaO > water consumption > Na_3PO_4 > Na_2CO_3. Therefore, this study provides a new method for low-cost process disposal and efficient harmless treatment of EMR (Reviewer #3).

Graphical Abstract

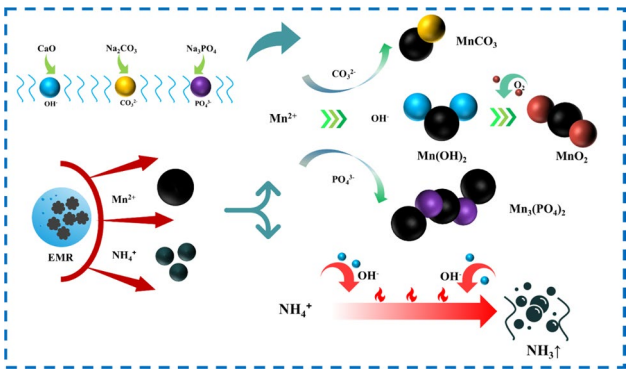

Keywords Low temperature thermochemistry · Electrolytic manganese residue · Harmless treatment · Solidification of soluble manganese · Ammonium ion removal (Reviewer #3)

Responsible Editor: Guilherme Luiz Dotto

Extended author information available on the last page of the article

Introduction

Manganese stands as an exceptionally vital industrial raw material, with manganese-containing alloy products finding extensive applications in non-ferrous metallurgy, electronics, chemicals, and various other industries (Ghosh et al. 2016). Presently, China holds the distinction of being the world's foremost producer, consumer, and exporter of electrolytic manganese metal (EMM), contributing over 97% to the global production (Du et al. 2014). Electrolytic manganese residue (EMR), a byproduct of manganese carbonate sulfuric acid leaching, ammonia water neutralization, and pressure filtration in EMM plants, poses a significant environmental challenge (He et al. 2021a) (Reviewer #3). Each ton of EMM production generates approximately 10–12 tons of EMR (Wang et al. 2016), resulting in an annual emission of around 10 million tons of EMR from Chinese EMM plants. This issue is exacerbated by the declining manganese ore grades, leading to an escalating yearly increase in EMR production, with the current volume exceeding 120 million tons (Shu et al. 2018).

To date, a substantial portion of EMR has been directly deposited in slag yards without proper pretreatment, causing severe harm to local ecological environments and impeding the global EMM industry's progress. The pollutants NH_4^+-N and Mn^{2+} in EMR pose a threat by infiltrating nearby soil and migrating to groundwater (Shu et al. 2016a).

Once the high concentration of ammonia nitrogen flows into the surrounding water environment, it will cause eutrophication of the water body (Zhang et al. 2020; Zulkifli et al. 2022), resulting in the excessive growth of microorganisms and algae and the depletion of dissolved oxygen in the water, so that a large number of aquatic organisms are anoxic and die (Yan et al. 2020), resulting in the destruction of ecological balance (Zhang et al. 2020). In addition, excessive ammonia nitrogen in the human body can also lead to blue baby syndrome, stomach and liver damage (Shu et al. 2019a). Drinking water contaminated with manganese may cause manganism, hallucinations, amnesia and nerve damage (Yang et al. 2022). At the same time, manganese can also lead to bronchitis, muscle weakness, headache, insomnia, even lead to schizophrenia (Hui et al. 2023), and potential risks to human health (Liu et al. 2017; Dey et al. 2022) (Reviewer #3).

Recognizing these risks, government bodies and relevant enterprises have closely monitored the issue since 2021. HJ 1241–2022 mandates that EMR must be 100% harmless before comprehensive utilization (Agency 2022), with the Ministry of Ecology and Environment setting a deadline for all disposal to be completed by 2025. Therefore, harmless disposal is imminent. Currently, research on the harmless treatment of EMR is ongoing. Fang (2014), Zhao et al (2017) have explored the washing method, which includes traditional slurry washing, slurry filter cake washing, and filtration combined with washing, effectively removing NH_4^+-N and Mn^{2+} from EMR. However, this method is not suitable for insoluble substances and increases the cost of treating waste liquid. Tian et al (2019) (Reviewer #3), Shu et al (2016b), investigated electric field-enhanced leaching and electrokinetic remediation, which effectively removes soluble manganese and ammonia nitrogen but has drawbacks such as long reaction times and high energy consumption (Liu et al 2020) (Reviewer #3).

Additionally, the chemical solidification method, a primary approach for treating toxic and hazardous solid waste (He et al. 2021b) (Reviewer #3), involves encapsulating pollutants in solid waste with inert or cementitious materials to create stable compounds (Li et al. 2023) (Such as cement (Liu et al. 2023), oligomers (Guo et al. 2017), etc.) (Reviewer #3). Luo et al (2017) studied EMR treatment by adding quicklime, but a lengthy standing time was required. Shu et al (2018; 2020) used alkaline materials and phosphate to immobilize soluble manganese and ammonia nitrogen simultaneously, yet faced challenges with a 48-h reaction time. Du et al (2015a; b) employed CaO and $NaHCO_3$ for synergistic solidification of Mn^{2+} in EMR, with a prolonged reaction and drying cycle. In light of the current research, there remains a lack of an efficient (short reaction time) and widely implemented method for achieving the harmless pretreatment standard of EMR before comprehensive utilization.

In summary, in order to explore the precise, efficient and harmless treatment methods of EMR, this study proposes a low-temperature thermochemical method to pretreat EMR, and uses three different alkaline reagents (quicklime, sodium carbonate, sodium phosphate) to ensure the accuracy and efficiency of harmless treatment. The main research contents are as follows: The samples are heated at low temperature (40~100 ℃), and the EMR is harmlessly treated by chemical reaction at this temperature. The impact of factors such as reaction temperature, time, lime dosage, sodium carbonate dosage, sodium phosphate dosage, and water consumption on EMR's harmless treatment effectiveness. The primary indicators for harmlessness are to reduce the ammonium ion and soluble manganese content in the solid. (Reviewer #4) This study provides a new method for the low-cost process disposal and efficient harmless treatment of EMR, and can provide effective support for the EMR harmless treatment production line, and promote the next resource utilization after EMR pretreatment (Reviewer #3).

Materials and methods

Materials

The EMR utilized in the experiment originated from an electrolytic manganese plant in Quanzhou, Guilin, Guangxi, China (111° 05′ 38.21″ E, 25° 57′ 47.85″ N) (Reviewer #3), displaying a black mud paste appearance (Zhou et al. 2023) (Reviewer #3). Table 1 presents the results obtained through X-ray fluorescence spectrometry (XRF, ZSX Primus II) (Reviewer #3) analysis of the electrolytic manganese residue. Prior to conducting the harmless experiment, the EMR samples underwent drying to a constant weight at 60 ℃ (Reviewer #3). Subsequently, the dried EMR underwent grinding using a ball mill and sieving through a 100-mesh sieve, with a sieve margin of less than 2%. The analytical chemical reagents (purity ≥ 99.7%) (Reviewer #3) employed in the experiment included lime (CaO), sodium carbonate (Na_2CO_3), and sodium phosphate dodecahydrate ($Na_3PO_4{\cdot}12H_2O$). These reagents were purchased from Xilong Scientific Co., Ltd (Reviewer #3). Deionized water was utilized in the experiments as well.

The results of X-ray diffraction (XRD, X′Pert PRO) experiments which are shown in Fig. 1. on EMR (Reviewer #3). The mineral components present in electrolytic manganese residue, as illustrated in Fig. 1, primarily consist of $CaSO_4{\cdot}2H_2O$ (dihydrate gypsum), SiO_2 (quartz), $(NH_4)[Fe_3(OH)_6(SO_4)_2]$ (ammonium jarosite), $Fe(NH_4)_2(SO_4)_2{\cdot}6H_2O$ (Ammonium iron sulfate), $MnFeO_2$ (Manganese ferrite), $(NH_4)_2Mn(SO_4)_2$ (ammonium manganous sulfate), FeO(OH) (Iron hydroxide oxide) (Reviewer #3) and others. Notably, the characteristic spectral lines of $CaSO_4{\cdot}2H_2O$ and SiO_2 exhibit sharpness, indicating good crystallinity (Wu et al. 2024) (Reviewer #3). The characteristic peak of $(NH_4)[Fe_3(OH)_6(SO_4)_2]$ is distinct and exhibits a certain degree of crystallinity. $CaSO_4{\cdot}2H_2O$ originates from the reaction between $CaCO_3$ and sulfuric acid (H_2SO_4) during the acid leaching process of rhodochrosite (Su et al. 2023) (Reviewer #3). The chemical formula is as follows (1) (Reviewer #3):

$$CaCO_3 + H_2SO_4 + H_2O \rightarrow CaSO_4 \cdot 2H_2O + CO_2 \quad (1)$$

Compounds such as $(NH_4)_2Mn(SO_4)_2$, $Fe(NH_4)_2(SO_4)_2{\cdot}6H_2O$, $MnFeO_2$, among others, suggest that after the rhodochrosite leaching, the Mn^{2+} not completely filtered out and the ammonia added to adjust the pH are transferred to the electrolytic manganese residue during the subsequent pressure filtration process (Duan et al. 2010).

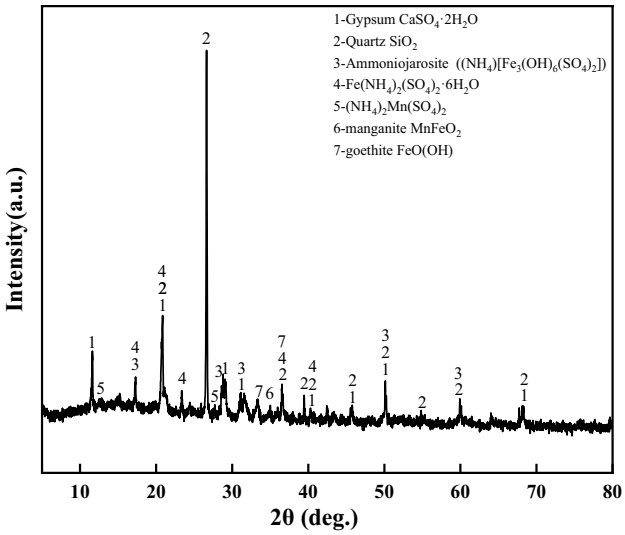

Fig. 1 XRD pattern of EMR

In this study, EMR undergoes a harmless treatment using low-temperature heating and thermochemical methods, as illustrated in Fig. 2. (Reviewer #3) After drying and grinding, the EMR is mixed with the corresponding reagent in the mixing tank, and then the appropriate amount of water is added to the reaction vessel to react to the corresponding time to obtain the harmless sample (Reviewer #4).

Experimental

The experimental parameters are as follows: the reaction temperature is set at 40, 60, 80, and 100 °C, and the reaction time is varied between 5, 10, 15, 20 min. (Note: Due to the sample's thinness, sampling at 40 °C is performed from 25 min onwards.) The reagent dosage is adjusted to 0%, 3%, 6%, 9%, and 12%, respectively, as outlined in Table 2. The investigation into the harmless treatment efficiency of EMR covers four key aspects: CaO, Na_2CO_3, Na_3PO_4, and water consumption (Shu et al. 2020) (Reviewer #3). The corresponding ratios are detailed in Tables 3, 4, 5, and 6.

Analysis and detection methods

(1) Determination of EMR Moisture Content: The assessment was conducted in accordance with GB/T 14949.8 (Agency 2018). The recorded average moisture content stands at 17%.

Table 1 EMR composition of raw materials, wt.%

Raw materials	SiO_2	SO_3	Fe_2O_3	CaO	Al_2O_3	MnO	MgO	P_2O_5	Others
EMR	35.53	16.60	22.53	8.04	5.29	7.35	1.90	0.83	1.93

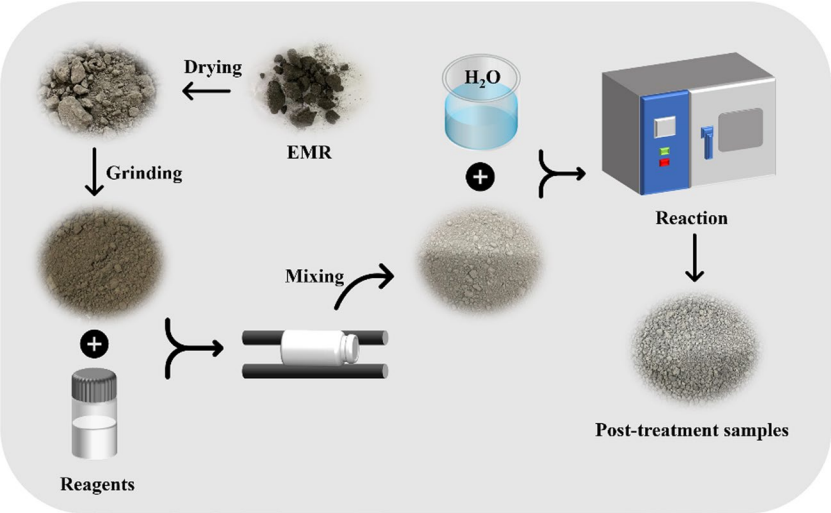

Fig. 2 Schematic diagram of harmless treatment of EMR (Reviewer #3)

Table 2 Reaction Temperature, Time Experimental Ratio, wt.%

Number	CaO (%)	Na_2CO_3 (%)	Na_3PO_4 (%)	W (%)
1	10	1	0.5	80

Table 3 CaO in electrolytic manganese residue Addition ratio, wt.%

Number	CaO(%)	Na_2CO_3 (%)	Na_3PO_4 (%)	W (%)
Ca-0	0	2	2	40
Ca-3	3			
Ca-6	6			
Ca-9	9			
Ca-12	12			

Table 4 Na_2CO_3 in EMR Addition ratio, wt.%

Number	CaO (%)	Na_2CO_3 (%)	Na_3PO_4 (%)	W (%)
N2-0	3	0	2	40
N2-3		3		
N2-6		6		
N2-9		9		
N2-12		12		

Table 5 Na_3PO_4 in EMR Addition ratio, wt.%

Number	CaO(%)	Na_2CO_3(%)	Na_3PO_4(%)	W(%)
N3-0	3	2	0	40
N3-3			3	
N3-6			6	
N3-9			9	
N3-12			12	

Table 6 Water in EMR Addition ratio, wt.%

Number	CaO(%)	Na_2CO_3(%)	Na_3PO_4(%)	W(%)
W-3	6	2	2	30
W-5				50
W-7				70
W-9				90
W-12				120

(2) Referring to GB / T 39701 (Agency 2020), the standard ammonium ion limit was 210 mg/kg, and the content of EMR ammonium ion was 6101.88 mg/kg (Reviewer #3).

(3) The soluble manganese content was 1784 mg / L measured by EMR according to HJ 766 (Agency 2015). The samples to be tested were leached of soluble manganese ions (Mn^{2+}) according to HJ 557 (Agency 2010). A fitting curve correlating absorbance and soluble manganese content was generated according to GB 11906 (Agency 1989) (refer to Fig. 3). According to the curve, the content of soluble manganese was obtained. It is noteworthy that the soluble manganese content of harmless samples should not exceed the 2 mg/L limit specified in GB 8978 (Agency 1996) (Reviewer #3).

(4) XRD Analysis: The samples underwent analysis using an X'Pert PRO X-ray diffractometer, employing Cu target Kα-ray (λ = 1.54060 Å). The scanning angle range covered 5° to 80°, with a scanning duration of 4 min (Li et al. 2022). (Reviewer #3).

(5) SEM–EDS Characterization: Microstructure characterization and energy spectrum analysis of the samples were conducted using the FESM S-4800 (Li et al. 2022). (Reviewer #3).

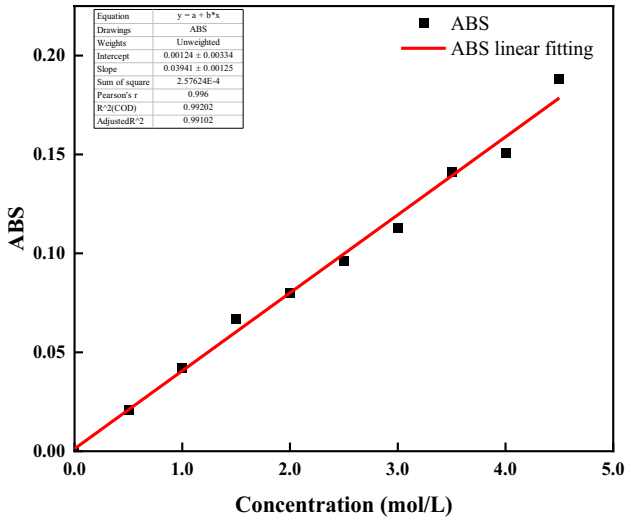

Fig. 3 Mn^{2+} concentration versus absorbance linear fitting curve

Result and Discussion

The effects of reaction temperature and reaction time on the removal of ammonia from (Reviewer #4) EMR were studied

Figure 4 (a) and (b) illustrate the impact of reaction temperature and reaction time on ammonia removal by EMR. Maintaining a specify values (Reviewer #3) an observable decrease in the levels of ammonium ions and soluble manganese in the sample is evident with the progression of both reaction temperature and reaction time. Regarding ammonia removal, higher temperatures correspond to a more significant reduction in ammonium ions in the initial stages. This phenomenon can be attributed to the accelerated volatilization of NH_4^+ into NH_3 under alkaline conditions as the temperature rises (Deng et al. 2018). (Reviewer #3).

Concerning manganese fixation, the soluble manganese content remains extremely low at this specify values (Reviewer #3). This observation underscores the notion that, within the context of the harmless EMR process, the challenge of ammonia removal surpasses that of manganese fixation. Notably, at a reaction temperature of 60 °C and a reaction time of 10 min, the ammonium ion content is measured at 93.29 mg/kg, yielding an impressive removal efficiency of 98.5%, well below the national standard limit of 210 mg/kg (Agency 2020) (Reviewer #3). Simultaneously, the soluble manganese content is a mere 0.07 mg/L, attaining an exceptional curing rate of 99.9%. Considering these factors comprehensively, this specific combination of reaction temperature and time is deemed optimal and is consequently selected for subsequent experiments.

Effect of CaO addition on manganese fixation and ammonia removal of EMR

Figure 5 (a) and (b) show the effect of lime addition on EMR manganese fixation and ammonia removal. Under the premise of constant Na_2CO_3, Na_3PO_4 and water consumption, with the increase of CaO content (0%, 3%, 6%, 9%, 12%) (Reviewer #3), the removal rate of ammonia nitrogen and the solidification rate of soluble manganese are significantly improved.

In Fig. 5 (a), the increase in CaO content correlates with a linear decrease in ammonium ions, declining from the initial level of 5536.48 mg/kg to 205.39 mg/kg. At this point, the ammonium ion content aligns with the stipulated limit of 210

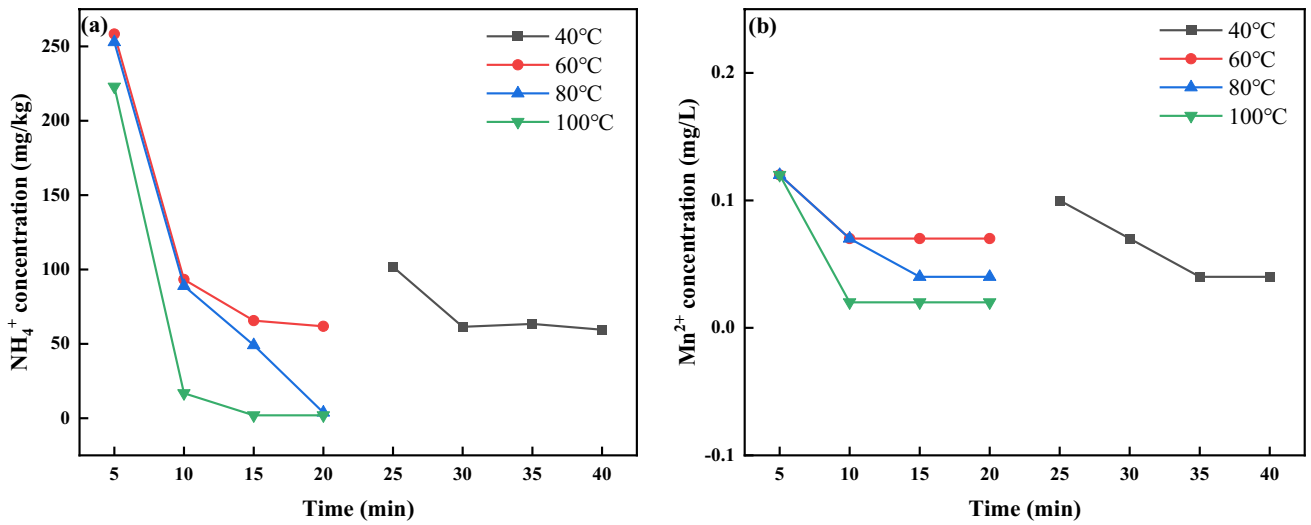

Fig. 4 Effect of reaction temperature and time on the content of ammonium ions (**a**) and soluble manganese (**b**) in EMR

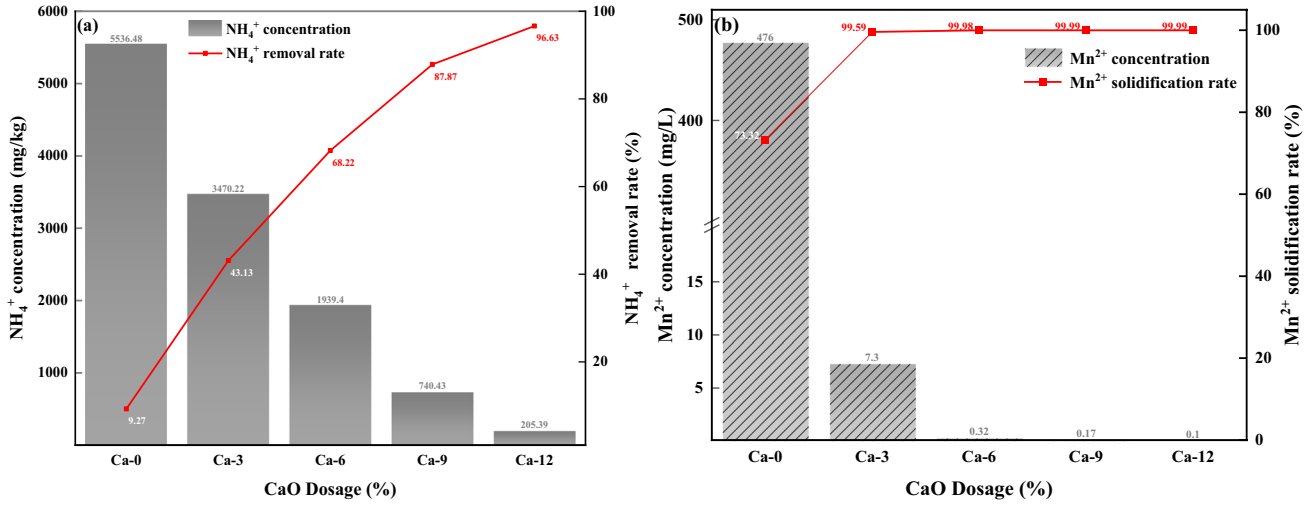

Fig. 5 Effect of CaO addition on the content of ammonium ion (**a**) and soluble manganese (**b**) in EMR (reaction temperature: 60 ℃ and reaction time: 10 min) (Reviewer #4)

mg/kg outlined in GB/T 39701 (Agency 2020) (Reviewer #3). The removal of ammonium ions is attributed to the escape of NH_4^+ in EMR in the form of NH_3 through the generation of OH^- resulting from the reaction between CaO and water (Zhou et al. 2013). The reaction equation is presented as follows (2~3) (Reviewer #3). Additionally, due to the exothermic nature of the CaO-water reaction and the low-temperature heating environment, this reaction proceeds swiftly.

$$CaO + H_2O \rightarrow Ca(OH)_2 \tag{2}$$

$$NH_4^+ + OH^- \xrightarrow{\Delta} NH_3 \uparrow \tag{3}$$

In Fig. 5 (b), as the CaO content increases, the concentration of Mn^{2+} undergoes a substantial reduction from 1784 mg/L to 0.1 mg/L. Specifically, when the CaO content reaches 6%, the Mn^{2+} concentration diminishes to 0.32 mg/L, complying with the specified limit of 2.0 mg/L in GB 8978 (Agency. 1996) (Reviewer #3). The primary mechanism behind this phenomenon is the formation of $Mn(OH)_2$ precipitation by Mn^{2+} under the alkaline conditions facilitated by CaO. Subsequently, $Mn(OH)_2$ undergoes oxidation by O_2 in the air, leading to the formation of stable compounds such as MnOOH, Mn_2O_3, and MnO_2 (Luo et al. 2017). The reaction equation, presented below (4~7) (Reviewer #3), illustrates how this process achieves the goal of solidifying soluble Mn^{2+}.

$$Mn^{2+} + 2OH^- \rightarrow Mn(OH)_2 \downarrow \tag{4}$$

$$4Mn(OH)_2 + O_2 \rightarrow 4MnOOH + 2H_2O \tag{5}$$

$$6Mn(OH)_2 + O_2 \rightarrow 2Mn_3O_4 + 6H_2O \tag{6}$$

$$2Mn(OH)_2 + O_2 \rightarrow 2MnO_2 + 2H_2O \tag{7}$$

In examining the XRD results presented in Fig. 6, it is evident that during the low-temperature thermochemical treatment of EMR, a portion of dihydrate gypsum ($CaSO_4{\cdot}2H_2O$) undergoes conversion into hemihydrate gypsum ($CaSO_4{\cdot}0.5H_2O$), as revealed through phase analysis. This transformation is likely attributed to the increased temperature inducing a change in the crystal form of gypsum (Duan et al. 2023) (Reviewer #3). Furthermore, the augmentation of CaO content correlates with a decrease in the crystallinity of $(NH_4)_2Mn(SO_4)_2$ and $Fe(NH_4)_2(SO_4)_2{\cdot}6H_2O$

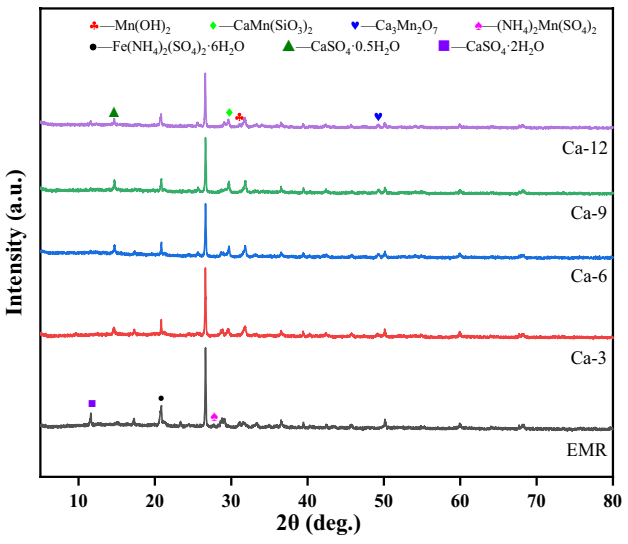

Fig. 6 XRD plots of samples harmless to EMR with different CaO additions

in EMR. This change is possibly linked to the escape of ammonium ions in the form of NH_3 under alkaline conditions (Zhang et al. 2023) (Reviewer #3), leading to alterations in these two phases (He et al. 2022) (Reviewer #3). Additionally, there is a discernible shift in the form of soluble manganese, characterized not only by the formation of $Mn(OH)_2$ precipitation but also by manganese binding with Ca^{2+} and SiO_3^{2-} to create stabilizers like $CaMn(SiO_3)_2$, $Ca_3Mn_2O_7$, and others (He et al. 2022). The corresponding reaction equations are provided below (8~10) (Reviewer #3).

$$SiO_2 + 2OH^- \rightarrow SiO_3^{2-} + H_2O \quad (8)$$

$$Ca^{2+} + 2SiO_3^{2-} + Mn^{2+} \rightarrow CaMn(SiO_3)_2 \downarrow \quad (9)$$

$$6Ca^{2+} + 4Mn^{2+} + 7O_2 \rightarrow 2Ca_3Mn_2O_7 \downarrow \quad (10)$$

Effect of Na_2CO_3 content on manganese fixation and ammonia removal of EMR

Figure 7 (a) and (b) depict the impact of sodium carbonate addition on EMR manganese fixation and ammonia removal. Maintaining constant CaO, Na_3PO_4, and water consumption, the rise in Na_2CO_3 content notably enhances the solidification rate of soluble manganese. However, the effect on ammonia removal is not as pronounced as observed with CaO.

In Fig. 7 (a), the increase in Na_2CO_3 content correlates with a substantial decrease in ammonium ion content, dropping from 3502.41 mg/kg to 1630.89 mg/kg. At a dosage of 12%, the removal rate reaches 73.27%, although the ammonium ion content still falls short of the stipulated limit of 210 mg/kg in GB/T 39701 (Agency. 2020) (Reviewer #3). This phenomenon can be attributed to the alkalinity provided by Na_2CO_3 still influencing EMR ammonia removal, albeit to a lesser extent compared to CaO, resulting in a limited effect (Li et al. 2018) (Reviewer #3).

In Fig. 7 (b), the elevation of Na_2CO_3 content leads to a significant reduction in the concentration of Mn^{2+}, decreasing from 18.4 mg/L to 0.04 mg/L. At a Na_2CO_3 content of 3%, the Mn^{2+} concentration diminishes to 0.7 mg/L, meeting the specified limit of 2.0 mg/L in GB 8978 (Agency. 1996) (Reviewer #3). The primary mechanism behind this observation is the formation of insoluble $MnCO_3$ (Du et al. 2015a) when Mn^{2+} combines with CO_3^{2-} under alkaline conditions. The corresponding reaction equation is provided below (11) (Reviewer #3), illustrating how this process achieves the desired effect of mitigating soluble Mn^{2+}.

$$Mn^{2+} + CO_3^{2-} \rightarrow MnCO_3 \downarrow \quad (11)$$

Examining Fig. 8, it is evident through phase analysis that, consistent with prior findings, some dihydrate gypsum ($CaSO_4 \cdot 2H_2O$) undergoes conversion into hemihydrate gypsum ($CaSO_4 \cdot 0.5H_2O$). Furthermore, with the inclusion of Na_2CO_3, the appearance of the characteristic peak of $MnCO_3$ aligns with previous analyses (Du et al. 2015a) (Reviewer #3), indicating that soluble manganese is fixed in the form of $MnCO_3$. Additionally, as Na_2CO_3 content increases, the characteristic peak of $CaCO_3$ emerges. This occurrence may be attributed to the fact that the solubility product constant (K_{sp}) of $MnCO_3$ ($K_{sp}(MnCO_3) = 1.8 \times 10^{-11}$) is significantly lower than that of $CaCO_3$ ($K_{sp}(CaCO_3) = 2.8 \times 10^{-9}$). Consequently, in the harmless treatment process, $MnCO_3$ precipitate

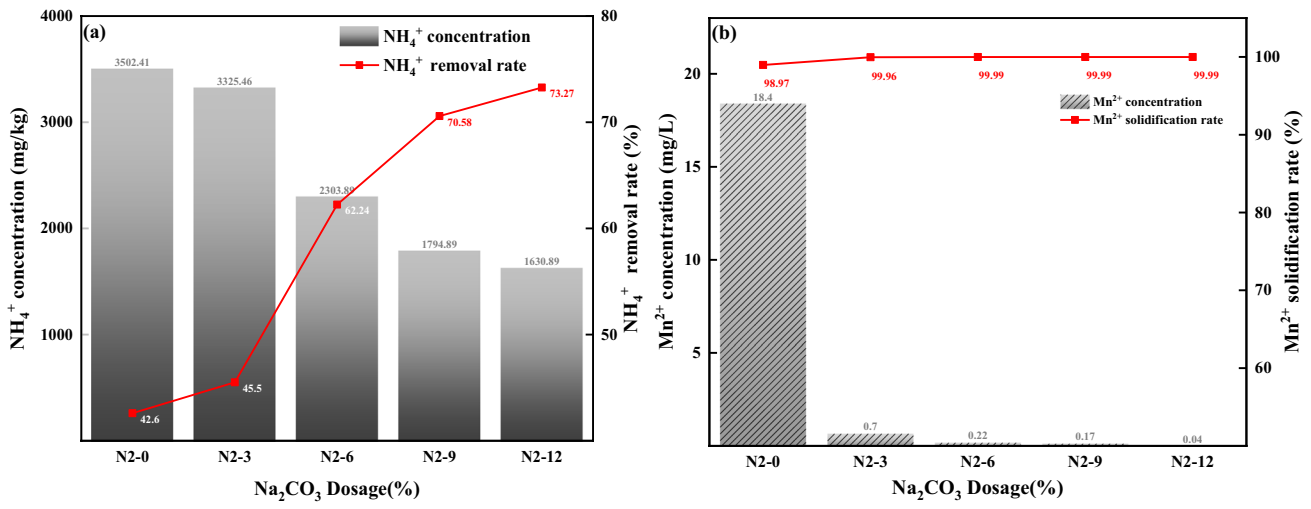

Fig. 7 Effect of Na_2CO_3 addition on the content of ammonium ion (**a**) and soluble manganese (**b**) in EMR (reaction temperature: 60 ℃ and reaction time: 10 min) (Reviewer #4)

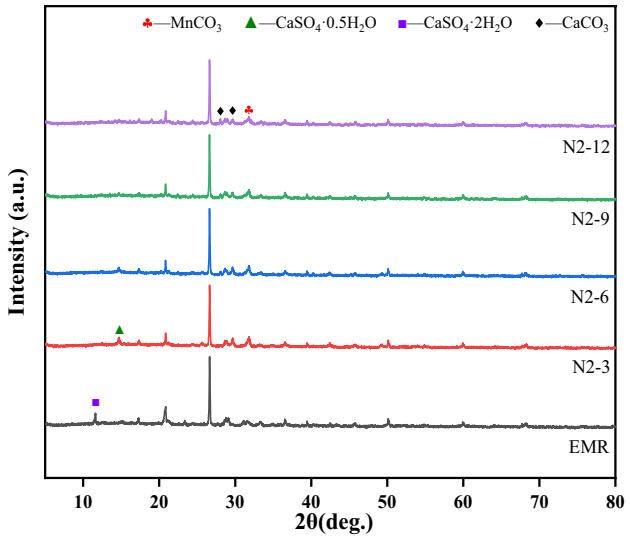

Fig. 8 XRD plots of samples harmless to EMR with different Na_2CO_3 additions

forms first (Li et al. 2021). Subsequently, the excess CO_3^{2-} in Na_2CO_3 reacts with Ca^{2+} in EMR to form $CaCO_3$ precipitate. The reaction equation representing this process is provided below (12) (Reviewer #3).

$$Ca^{2+} + CO_3^{2-} \rightarrow CaCO_3 \downarrow \quad (12)$$

Effect of Na_3PO_4 content on manganese fixation and ammonia removal of EMR

Figure 9 (a) and (b) illustrate the impact of sodium phosphate addition on EMR manganese fixation and ammonia removal. Under constant CaO, Na_2CO_3, and water consumption, the increase in Na_3PO_4 content exhibits a discernible, albeit less pronounced, effect on the removal of EMR ammonium ions and the solidification of soluble manganese compared to CaO and Na_2CO_3.

In Fig. 9 (a), the rise in Na_3PO_4 content leads to a noticeable decrease in ammonium ion content, dropping from 3571.92 mg/kg to 2039.57 mg/kg. At a dosage of 12%, the removal rate reaches 66.57%, yet the ammonium ion content still falls short of the stipulated limit of 210 mg/kg in GB/T 39701 (Agency. 2020) (Reviewer #3). The primary reason for this occurrence is that the weak alkalinity provided by Na_3PO_4 influences EMR ammonia removal, albeit to a lesser extent than CaO, resulting in a limited effect (Shu et al. 2019b) (Reviewer #3).

In Fig. 9 (b), the augmentation of Na_3PO_4 content significantly reduces the concentration of Mn^{2+}, decreasing from 9.8 mg/L to 0.15 mg/L. At a Na3PO4 content of 3%, the Mn^{2+} concentration diminishes to 0.7 mg/L, meeting the specified limit of 2.0 mg/L in GB 8978 (Agency. 1996) (Reviewer #3). The primary mechanism behind this observation is the formation of insoluble $Mn_3(PO_4)_2$ when Mn^{2+} combines with PO_4^{2-} under alkaline conditions (Chen et al. 2019). The corresponding reaction equation is provided below (13) (Reviewer #3), illustrating how this process achieves the desired effect of mitigating soluble Mn^{2+}. Concurrently, a comparison between N3-0 and N2-0, as well as Ca-0 groups, indicates that the curing effect of Na_3PO_4 on

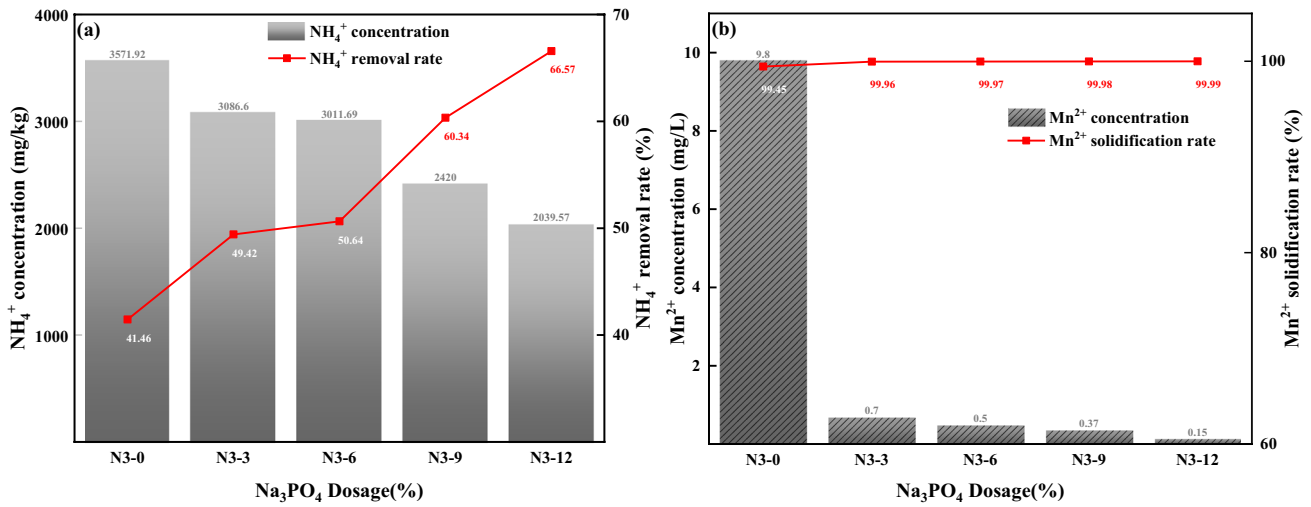

Fig. 9 Effect of Na_3PO_4 addition on the content of ammonium ion (**a**) and soluble manganese (**b**) of EMR (reaction temperature: 60 ℃ and reaction time: 10 min) (Reviewer #4)

soluble Mn^{2+} is not as effective as Na_2CO_3, suggesting a potential reduction in its dosage in subsequent experiments.

$$3Mn^{2+} + 2PO_4^{2-} \rightarrow Mn(PO_4)_2 \downarrow \quad (13)$$

The XRD of EMR harmless samples with raw residue and Na_3PO_4 content is shown in Fig. 10. Through phase analysis, in addition to the transformation of dihydrate gypsum ($CaSO_4{\cdot}2H_2O$) and hemihydrate gypsum ($CaSO_4{\cdot}0.5H_2O$), the characteristic peak of $Mn_3(PO_4)_2{\cdot}3H_2O$ appeared, which is consistent with the previous analysis (Chen et al. 2019) (Reviewer #3). Soluble manganese and PO_4^{2-} combined to form insoluble $Mn_3(PO_4)_2$ precipitation to achieve the purpose of curing soluble manganese.

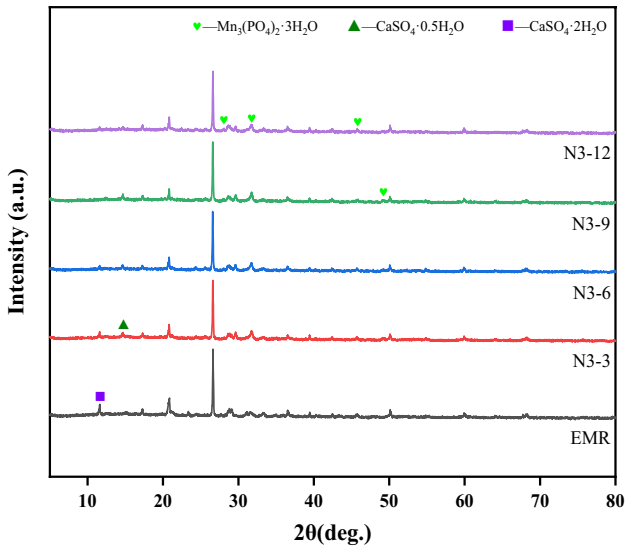

Fig. 10 XRD plots of samples harmless to EMR with different Na_3PO_4 additions

Effect of water addition on manganese fixation and ammonia removal of EMR

Figure 11(a) and (b) illustrate the impact of water consumption on EMR manganese fixation and ammonia removal. Maintaining constant levels of CaO, Na_2CO_3, and Na_3PO_4, the variations in water consumption exert a discernible effect on the removal of EMR ammonium ions and the solidification of soluble manganese.

In Fig. 11(a), as water consumption increases, there is a substantial initial decrease in ammonium ions in EMR. However, beyond a water consumption level of 70%, the reduction in ammonium ions becomes marginal. This phenomenon arises because the heightened water content affects the degree of ion interaction, but there is a discernible upper limit. Further increasing water volume beyond this point does not significantly enhance the removal of ammonium ions in EMR.

In Fig. 11(b), with a constant reagent dosage, the concentration of Mn^{2+} remains consistently low, meeting the specified limit of 2.0 mg/L in GB 8978 (Agency. 1996) (Reviewer #3). As water consumption increases, there is a modest improvement in the manganese fixation efficiency of the sample. This is attributed to the fact that water content also impacts the degree of ion reaction.

Figure 12 displays the XRD results of EMR harmless samples influenced by raw slag and water consumption. Through phase analysis, it becomes evident that as water consumption increases, the characteristic peak intensity of dihydrate gypsum ($CaSO_4{\cdot}2H_2O$) diminishes, concomitant

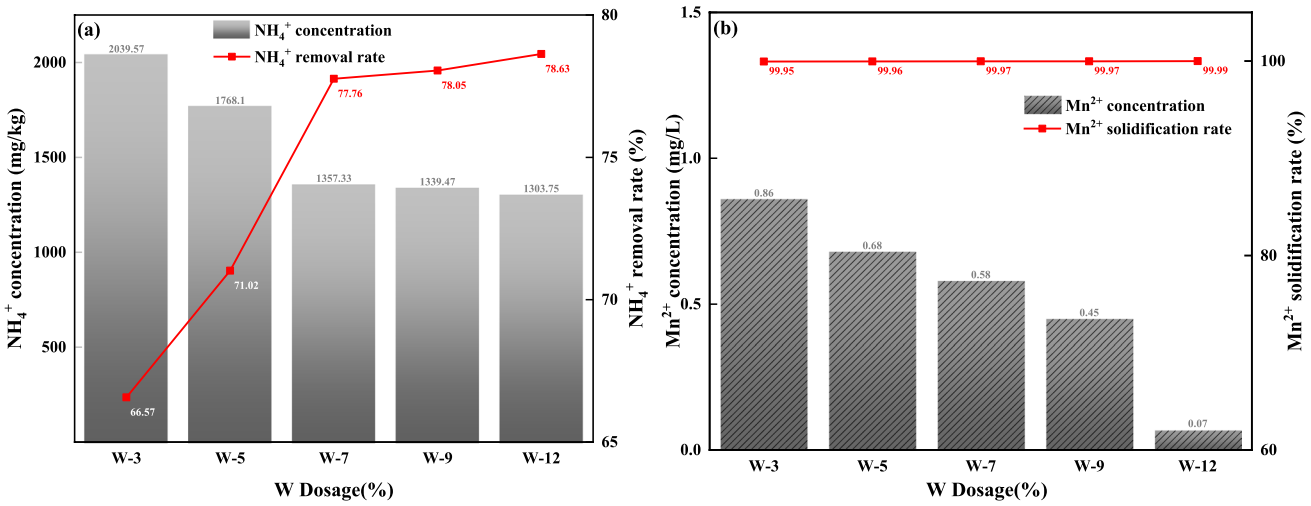

Fig. 11 Effect of water addition on the content of ammonium ion (**a**) and soluble manganese (**b**) in EMR (reaction temperature: 60 ℃ and reaction time: 10 min) (Reviewer #4)

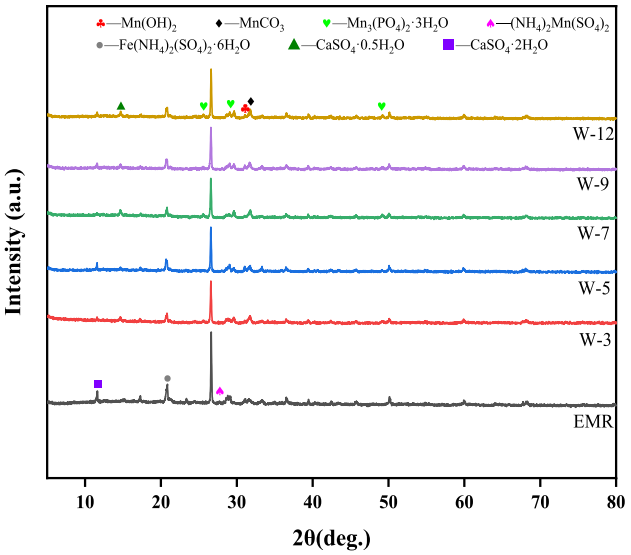

Fig. 12 XRD patterns of samples harmless to EMR with different water additions

with the appearance of the characteristic peak of hemihydrate gypsum ($CaSO_4{\cdot}0.5H_2O$). This observation may be attributed to the specific harmless treatment method employed in this study. Furthermore, the decrease in crystallinity of $(NH_4)_2Mn(SO_4)_2$ and $Fe(NH_4)_2(SO_4)_2{\cdot}6H_2O$ in EMR aligns with the aforementioned findings (Zhou et al. 2013) (Reviewer #3). Notably, the characteristic peak intensity of $Mn(OH)_2$, $MnCO_3$, and $Mn_3(PO_4)_2{\cdot}3H_2O$ increases with rising water consumption, underscoring that an elevated water content impacts the adequacy of ion reactions.

Orthogonal experiment

Through the conducted research, it becomes apparent that achieving the prescribed standard for the removal rate of ammonium ions is more readily accessible. However, for achieving the curing rate of soluble manganese at equivalent reagent dosages is more challenging. The impact of four variables impact on the removal degree of EMR ammonium ions was further investigated and the optimal mix ratio for harmless EMR was determined through an orthogonal experiment using L_9 (3^4) (Reviewer #3). The selected factor levels are as follows: CaO (6%, 8%, 10%), Na_2CO_3 (0.5%, 1%, 1.5%), Na_3PO_4 (0.5%, 1%, 1.5%), and water consumption (40%, 60%, 80%). The specific ratios are outlined in Table 7.

The evaluation indices for the orthogonal experiment were the ammonium ion content and soluble manganese content of the treated EMR, aiming to analyze the impact of each level factor on these two measures. The results of the orthogonal test and subsequent range analysis are presented in Tables 7 and 8. The greater the range (R value, $R=K_{avg}max\text{-}K_{avg}min$) (Reviewer #3), the more pronounced the influence of factors on the test results. Analyzing the K value corresponding to different levels of each factor helps identify the level closest to satisfactory test results for the index, facilitating the determination of the optimal level combination for each factor. (K value is the sum of experimental data at the same level of a certain factor. K_{avg} is the corresponding average, and the following values are the K_{avg}.) (Reviewer #3).

Table 7 R value (Reviewer #3) reveals that the lowest ammonium ion content in treated EMR was observed in Z-8 at 93.29 mg/kg. The ammonium ion content exhibited varying degrees of change with alterations in CaO, Na_3PO_4, Na_2CO_3, and water consumption. Notably, the curing rate of manganese ions in the orthogonal experimental group remained consistently high, underscoring the greater difficulty in achieving high removal of ammonium ions compared to achieving high curing of soluble manganese. Subsequently, the ammonium ion content was analyzed based on the results of the orthogonal test.

The interaction curve of the four factors Kavg in Table 8 is shown in Fig. 13. It can be seen from the figure that CaO and water consumption have a great influence on the removal

Table 7 Orthogonal experimental mix ratios and results wt.%

Number	A(CaO)	B(Na_2CO_3)	C(Na_3PO_4)	D(W)	NH_4^+ concentration (mg/kg)	NH_4^+ removal rate (%)	Mn^{2+} concentration (mg/L)	Mn^{2+} solidification rate (%)
Z-1	6	0.5	0.5	40	2197.14	63.99	0.18	99.84
Z-2	6	1	1	60	1516.01	75.16	0.1	99.91
Z-3	6	1.5	1.5	80	1498.42	75.44	0.07	99.93
Z-4	8	0.5	1	80	391.12	93.6	0.04	99.96
Z-5	8	1	1.5	40	1444.5	76.33	0.15	99.87
Z-6	8	1.5	0.5	60	666.83	89.07	0.12	99.89
Z-7	10	0.5	1.5	60	541.15	91.13	0.09	99.92
Z-8	10	1	0.5	80	93.29	98.47	0.07	99.94
Z-9	10	1.5	1	40	1284.10	78.96	0.09	99.92

Table 8 Effect of factors on ammonium ion content of EMR wt.%

Samples	NH_4^+ concentration (mg/kg)			
	A CaO (%)	B Na_2CO_3(%)	C Na_3PO_4(%)	D W(%)
K1	1737.19	1043.14	985.75	1641.91
K2	834.15	1017.93	1063.74	908.00
K3	639.51	1149.78	1161.36	660.94
R	1097.68	131.85	175.61	998.97

of ammonium ions in the sample. In order to ensure that the ammonium ion content of the sample is low, a high content of CaO and water consumption (10% CaO and 80% W) is required. On the contrary, Na_2CO_3 and Na_3PO_4 have little effect on the removal of ammonium ions in the sample, and the minimum value of K_{avg} can be taken (1% Na_2CO_3 and 0.5%Na_3PO_4). Therefore, Z-8 group is the best harmless group.

From the Table 8 R value, it can also be seen that the CaO content has the most significant effect on the removal effect of EMR ammonium ion (Reviewer #3), while Na_2CO_3 has a relatively minor impact on the removal effectiveness. The hierarchy of factors influencing the removal of ammonium ions by EMR is as follows: CaO > water consumption > Na_3PO_4 > Na_2CO_3. The dominant impact of CaO can be attributed to its high alkalinity, allowing for the rapid conversion of ammonium ions into ammonia volatilization under low-temperature heating conditions. The quantity of water accelerates ion reactions, with a more pronounced effect in dry reactions.

Conversely, the low alkalinity of Na_2CO_3 and Na_3PO_4 imparts a comparatively minor influence on the removal of ammonium ions by EMR. Notably, the higher removal of ammonium ions by Na_3PO_4 compared to Na_2CO_3 may stem from the complexation of $(PO_4)^{3-}$ with a small amount of NH_4^+ (Chen et al. 2019).

Based on the phase analysis of Z-8 and EMR in the qualified group, as depicted in Fig. 14, it becomes evident that the characteristic peak of $(NH_4)_2Mn(SO_4)_2$ disappears with the removal of ammonium ions. Mn^{2+} undergoes solidification, taking the forms of $Mn(OH)_2$, MnO_2, $MnCO_3$, and $Mn_3(PO_4)_2{\cdot}3H_2O$. Additionally, the characteristic peak of $CaSO_4{\cdot}0.5H_2O$ emerges due to the low-temperature thermochemical harmless method. The augmentation of the characteristic peak of $CaCO_3$ may be attributed to the reaction of OH^- with CO_2 in the air, resulting in the formation of CO_3^{2-}, which then reacts with Ca^{2+} to produce a $CaCO_3$ precipitate.

The SEM and EDS surface scan analysis in Fig. 15, comparing EMR samples (a, b, c) with the qualified group Z-8 (d, e, f), reveals distinctive features. In the EMR samples, irregular massive, columnar, and flaky substances identified as $CaSO_4{\cdot}2H_2O$ are observed, arranged alternately and disorderly stacked. Some irregular fine particles, likely composed of SiO_2 or other minerals rich in Al and Fe, may be attached to the $CaSO_4{\cdot}2H_2O$ structure (Xue et al. 2020). Post-harmless treatment, the EMR retains $CaSO_4{\cdot}2H_2O$, with an increase in small particles covering the surface of $CaSO_4{\cdot}2H_2O$. These small particles may be carbonates and hydroxide precipitates formed through the reaction of heavy metal ions with OH^- and CO_3^{2-} (Shu et al. 2020). This observation further underscores the efficacy of solidifying heavy metal ions in EMR during the harmless treatment process.

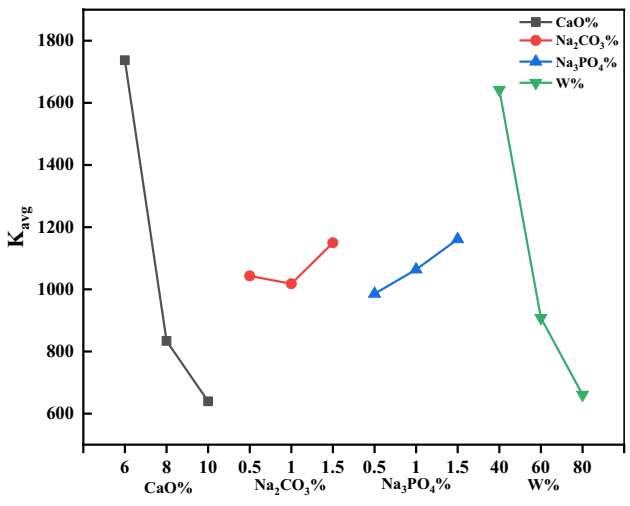

Fig. 13 The interaction curve diagram of various factors(Reviewer #3)

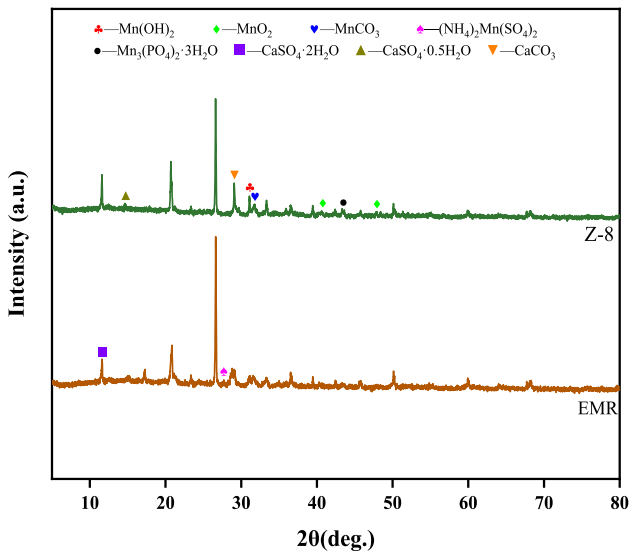

Fig. 14 XRD patterns of samples harmless to EMR

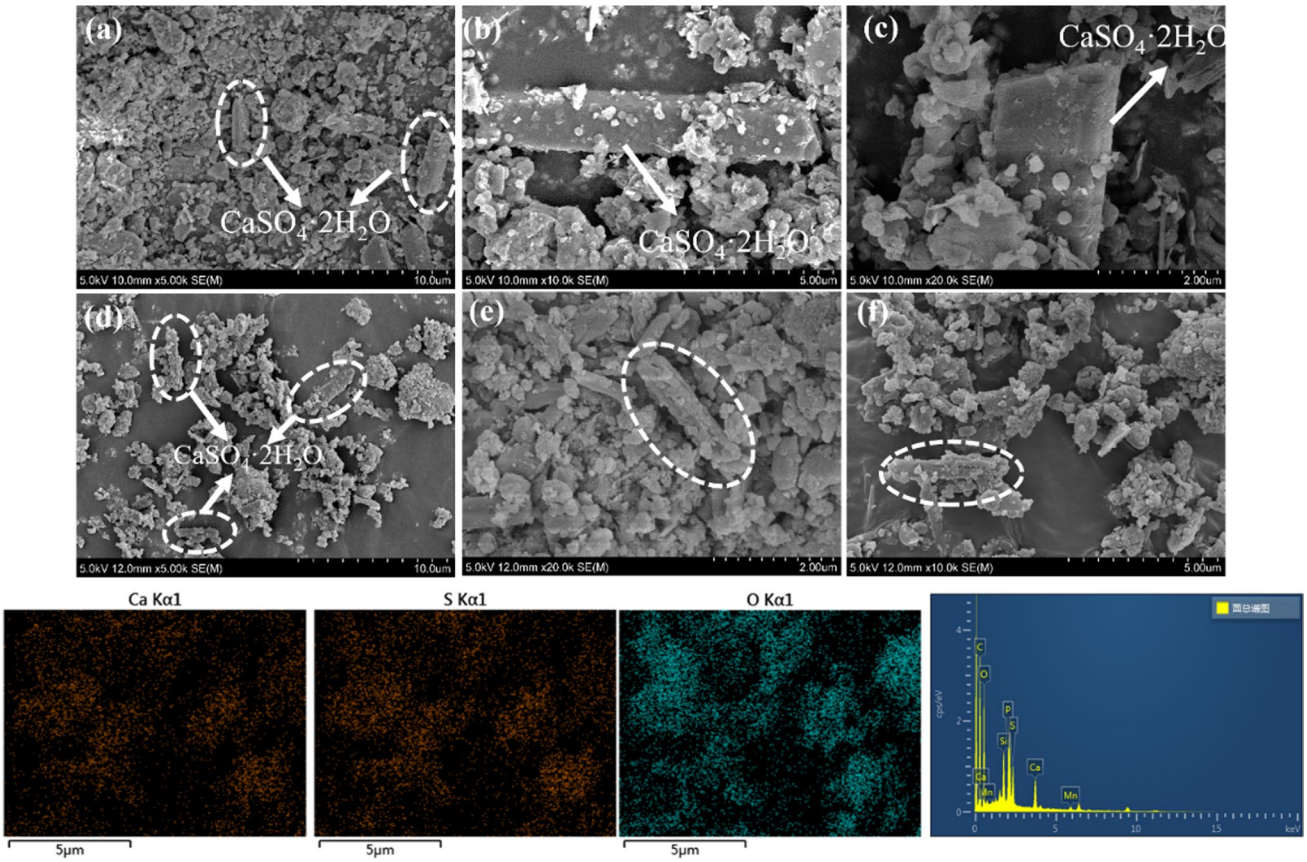

Fig. 15 SEM–EDS images of EMR and harmless to EMR samples

Conclusion

In this study, a low-temperature thermochemical method was employed to investigate the impact of reaction temperature, reaction time, CaO, Na_2CO_3, Na_3PO_4, and water consumption on the efficacy of EMR manganese fixation and ammonia removal. Orthogonal experiments were designed to assess the influence of four variables on the removal of EMR ammonium ions, ultimately leading to the identification of the optimal mix ratio. The key findings of the experiments are summarized as follows:

1) The increase in reaction temperature and reaction time facilitates ion reactions, resulting in a varying degree of reduction in ammonium ion and soluble manganese content in the sample. Considering all factors, a reaction temperature of 60 °C and a reaction time of 10 min were selected as the optimal conditions for achieving harmlessness.
2) The high alkalinity and substantial heat release provided by CaO in water not only efficiently remove ammonium ions in EMR but also solidify soluble Mn^{2+} in the form of precipitates, such as $Mn(OH)_2$, $CaMn(SiO_3)_2$, and $Ca_3Mn_2O_7$.
3) Na_2CO_3's alkalinity has a relatively low removal efficiency for EMR ammonium ions, but it exhibits good manganese fixation efficiency. This is attributed to the smaller $K_{sp}(MnCO_3)$ compared to $K_{sp}(CaCO_3)$, causing CO_3^{2-} to induce the formation of $MnCO_3$ precipitate. The addition of Na_3PO_4 induces Mn^{2+} to form $Mn_3(PO_4)_2 \cdot 3H_2O$ precipitation. The increase of water consumption promotes the reaction between ions(Reviewer #3).
4) In the orthogonal experiment, the order of influence of various factors on the removal of ammonium ions by EMR is CaO > water consumption > Na_3PO_4 > Na_2CO_3. Under The optimal mixing ratio(Reviewer #3), the ammonium ion content of the sample is 93.29 mg/kg, with a removal rate of 98.5%. The soluble manganese content is 0.07 mg/L, achieving a curing rate of 99.9%, well below the national standard limit.

This study addresses a new harmless process-low temperature thermochemical method was used to treat EMR efficiently and harmlessly, and solves the issue of EMR

pollution stemming from the EMM industry, providing novel research methodologies for the harmless treatment of EMR (Reviewer #3). It realizes an economical and efficient harmless treatment of EMR. The harmless products will be used for the resource utilization of supplementary cementitious materials and cement retarders (Reviewer #4). However, continued research on short-term and long-term curing properties, as well as cost control, is crucial, and ongoing attention to these areas is warranted.

Author contributions Zhihan Xie: conceptualization, date curation, formal analysis, investigation, methodology, software, original draft preparation, review, and editing. Rongjin Liu: conceptualization, project administration, methodology, review and editing, funding acquisition, resources. Fuhua Lu: methodology, conceptualization, project administration, review and editing. Daiyan Jing: conceptualization, methodology, project administration, review, and editing. Yanrong Zhao: conceptualization, review and editing. Jianbo Liang: conceptualization, investigation, software, validation. Wanyu Huang: software, date curation, validation. Yuhang Liu: methodology, software.

Funding This study was financially supported by Guangxi science and technology development strategy research project: science and technology support Guangxi solid waste new material industry development path and policy recommendations (Guike ZL23014014), 202305–202404.

Data availability statement The data are available from the corresponding author on reasonable request.

Declarations

Ethical approval and consent to participate Written informed consent for publication of this paper was obtained from all authors.

Consent to publish The work described has not been published before; that it is not under consideration for publication anywhere else; that its publication has been approved by all co-authors.

Competing interests The authors have no relevant financial or non-financial interests to disclose.

References

Agency NEP (1989) Water quality-determination of manganese-potassium periodate spectrophotometric method. Standard press of China, Beijing, China, pp GB 11906–89. http://www.csres.com/detail/83178.html

Agency NEP (1996) Integrated wastewater discharge standard. Standard press of China, Beijing, China, pp GB 8978–1996. http://www.csres.com/detail/70801.html

Agency NEP (2010) Solid waste-extraction procedure for leaching toxicity-horizontal vibration method. Standard press of China, Beijing, China, pp HJ 557–2010. http://www.csres.com/detail/209353.html

Agency NEP (2015) Solid waste-determination of metals-inductively coupled plasma mass spectrometry (ICP-MS). Standard press of China, Beijing, China, pp HJ 766–2015. http://www.csres.com/detail/277694.html

Agency NEP (2018) Manganese ores-determination of hygroscopic moisture content-gravimetric method. Standard press of China, Beijing, China, pp GB/T 14949.8–2018. http://www.csres.com/detail/319967.html

Agency NEP (2020) Limit and test method of ammonium ion content in fly ash. Standard press of China, Beijing, China, pp GB/T 39701–2020. http://www.csres.com/detail/356421.html

Agency NEP (2022) Technical specification for pollution control of manganese residue. Standard press of China, Beijing, China, pp HJ 1241–2022. http://www.csres.com/detail/378805.html

Chen H, Long Q, Zhang Y et al (2019) Simultaneous immobilization of NH4+ and Mn2+ from electrolytic manganese residue using phosphate and magnesium sources. RSC Adv 9(8):4583–4590. https://doi.org/10.1039/c8ra09615e

Deng Y, Li Y, Li L (2018) Experimental investigation of nitrogen isotopic effects associated with ammonia degassing at 0–70° C. Geochim Cosmochim Acta 226:182–191. https://doi.org/10.1016/j.gca.2018.02.007

Dey S, Charan SS, Pallavi U et al (2022) The removal of ammonia from contaminated water by using various solid waste biosorbents. Energy Nexus 7:100119. https://doi.org/10.1016/j.nexus.2022.100119

Du B, Zhou C, Dan Z et al (2014) Preparation and characteristics of steam-autoclaved bricks produced from electrolytic manganese solid waste. Constr Build Mater 50:291–299. https://doi.org/10.1016/j.conbuildmat.2013.09.055

Du B, Hou D, Duan N et al (2015a) Immobilization of high concentrations of soluble Mn(II) from electrolytic manganese solid waste using inorganic chemicals. Environ Sci Pollut Res 22(10):7782. https://doi.org/10.1007/s11356-015-4197-0

Du B, Zhou C, Li X et al (2015b) A kinetic study of Mn(II) precipitation of leached aqueous solution from electrolytic manganese residues. Toxicol Environ Chem 97(3–4):349–357. https://doi.org/10.1080/02772248.2015.1050188

Duan N, Fan W, Changbo Z et al (2010) Analysis of pollution materials generated from electrolytic manganese industries in China. Resour Conserv Recycl 54(8):506–511. https://doi.org/10.1016/j.resconrec.2009.10.007

Duan N, Cui K, Zhu C et al (2023) Study on phase evolution and promoting the pozzolanic activity of electrolytic manganese residue during calcination. Environ Res 227:115774. https://doi.org/10.1016/j.envres.2023.115774

Fang X (2014) Study on recovery process of soluble manganese and ammonium sulfate in electrolytic manganese residue. Guangi university. (in Chinese). https://doi.org/10.7666/d.Y3438529

Ghosh S, Mohanty S, Akcil A et al (2016) A greener approach for resource recycling: Manganese bioleaching. Chemosphere 154:628–639. https://doi.org/10.1016/j.chemosphere.2016.04.028

Guo B, Liu B, Yang J et al (2017) The mechanisms of heavy metal immobilization by cementitious material treatments and thermal treatments: A review. J Environ Manag 193:410–422. https://doi.org/10.1016/j.jenvman.2017.02.026

He D, Shu J, Wang R et al (2021a) A critical review on approaches for electrolytic manganese residue treatment and disposal technology: Reduction, pretreatment, and reuse. J Hazard Mater 418:126235. https://doi.org/10.1016/j.jhazmat.2021.126235

He S, Jiang D, Hong M et al (2021b) Hazard-free treatment and resource utilisation of electrolytic manganese residue: A review. J Clean Prod 306:127224. https://doi.org/10.1016/j.jclepro.2021.127224

He D, Shu J, Zeng X et al (2022) Synergistic solidification/stabilization of electrolytic manganese residue and carbide slag. Sci Total Environ 810:152175. https://doi.org/10.1016/j.scitotenv.2021.152175

Hui Y, Shihua W, Jianhua W (2023) Study on purification method of micro-polluted groundwater. E3S Web Conf 393:03018. https://doi.org/10.1051/e3sconf/202339303018. (EDP Sciences)

Li J, Du D, Peng Q et al (2018) Activation of silicon in the electrolytic manganese residue by mechanical grinding-roasting. J Clean Prod 192:347–353. https://doi.org/10.1016/j.jclepro.2018.04.184

Li Z, Guo B, Chen Y et al (2021) Optimized synthesis condition and mechanism for novel spherical cobalt-free 0.6Li2MnO3·0.4Li[Fe1/3Ni1/3Mn1/3]O2 cathode. J Power Sources 487:229410. https://doi.org/10.1016/j.jpowsour.2020.229410

Li J, Li Q, Chen P et al (2022) The Effect of Bayer Red Mud Blending on the Mechanical Properties of Alkali-Activated Slag-Red Mud and the Mechanism. Appl Sci 13(1):452. https://doi.org/10.3390/app13010452

Li W, Jin H, Xie H et al (2023) Progress in comprehensive utilization of electrolytic manganese residue: a review. Environ Sci Pollut Res 30(17):48837–48853. https://doi.org/10.1007/s11356-023-26156-5

Liu H, Zhu L, Tian X et al (2017) Seasonal variation of bacterial community in biological aerated filter for ammonia removal in drinking water treatment. Water Res 123:668–677. https://doi.org/10.1016/j.watres.2017.07.018

Liu R, Wang H, Liu Z et al (2020) Electrokinetic remediation with solar powered for electrolytic manganese residue and researching on migration of ammonia nitrogen and manganese. J Water Process Eng 38:101655. https://doi.org/10.1016/j.jwpe.2020.101655

Liu J, Wu D, Tan X et al (2023) Review of the Interactions between Conventional Cementitious Materials and Heavy Metal Ions in Stabilization/Solidification Processing. Materials 16(9):3444. https://doi.org/10.3390/ma16093444

Luo L, Jiang L, Zou H et al (2017) Harmless technology of manganese slag based on lime strengthening treatment (in Chinese) (6):4. https://doi.org/10.3969/j.issn.1007-7545.2017.06.016

Shu J, Liu R, Liu Z et al (2016a) Enhanced extraction of manganese from electrolytic manganese residue by electrochemical. J Electroanal Chem 780:32–37. https://doi.org/10.1016/j.jelechem.2016.08.033

Shu J, Liu R, Liu Z et al (2016b) Simultaneous removal of ammonia and manganese from electrolytic metal manganese residue leachate using phosphate salt. J Clean Prod 135:468–475. https://doi.org/10.1016/j.jclepro.2016.06.141

Shu J, Wu H, Liu R et al (2018) Simultaneous stabilization/solidification of Mn2+ and NH4+-N from electrolytic manganese residue using MgO and different phosphate resource. Ecotoxicol Environ Saf 148:220–227. https://doi.org/10.1016/j.ecoenv.2017.10.027

Shu J, Chen M, Wu H et al (2019a) An innovative method for synergistic stabilization/solidification of Mn^{2+}, NH_4^+-N, PO_4^{3-} and F^- in electrolytic manganese residue and phosphogypsum. J Hazard Mater 376:212–222. https://doi.org/10.1016/j.jhazmat.2019.05.017

Shu J, Wu H, Chen M et al (2019b) Simultaneous optimizing removal of manganese and ammonia nitrogen from electrolytic metal manganese residue leachate using chemical equilibrium model. Ecotoxicol Environ Saf 172:273–280. https://doi.org/10.1016/j.ecoenv.2019.01.071

Shu J, Li B, Chen M et al (2020) An innovative method for manganese (Mn^{2+}) and ammonia nitrogen (NH_4^+-N) stabilization/solidification in electrolytic manganese residue by basic burning raw material. Chemosphere 253:126896. https://doi.org/10.1016/j.chemosphere.2020.126896

Su H, Zhou W, Lyu X et al (2023) Remediation treatment and resource utilization trends of electrolytic manganese residue. Miner Eng 202:108264. https://doi.org/10.1016/j.mineng.2023.108264

Tian Y, Shu J, Chen M et al (2019) Manganese and ammonia nitrogen recovery from electrolytic manganese residue by electric field enhanced leaching. J Clean Prod 236:117708. https://doi.org/10.1016/j.jclepro.2019.117708

Wang N, Fang Z, Peng S et al (2016) Recovery of soluble manganese from electrolyte manganese residue using a combination of ammonia and CO2. Hydrometallurgy 164:288–294. https://doi.org/10.1016/j.hydromet.2016.06.019

Wu Z, Feng Z, Pu S et al (2024) Mechanical properties and environmental characteristics of the synergistic preparation of cementitious materials using electrolytic manganese residue, steel slag, and blast furnace slag. Constr Build Mater 411:134480. https://doi.org/10.1016/j.conbuildmat.2023.134480

Xue F, Wang T, Zhou M et al (2020) Self-solidification/stabilisation of electrolytic manganese residue: Mechanistic insights. Constr Build Mater 255:118971. https://doi.org/10.1016/j.conbuildmat.2020.118971

Yan Z, Zheng X, Fan J et al (2020) China national water quality criteria for the protection of freshwater life: Ammonia. Chemosphere 251:126379. https://doi.org/10.1016/j.chemosphere.2020.126379

Yang T, Xue Y, Liu X et al (2022) Solidification/stabilization and separation/extraction treatments of environmental hazardous components in electrolytic manganese residue: a review. Process Saf Environ Prot 157:509–526. https://doi.org/10.1016/j.psep.2021.10.031

Zhang R, Ma X, Shen X et al (2020) Life cycle assessment of electrolytic manganese metal production. J Clean Prod 253:119951. https://doi.org/10.1016/j.jclepro.2019.119951

Zhang J, Li R, Zhang Y et al (2023) Study on mutual harmless treatment of electrolytic manganese residue and red mud. Environ Sci Pollut Res 30(21):59660–59675. https://doi.org/10.1007/s11356-023-26752-5

Zhao B, Wang X, Zhu K et al (2017) Effects of washing methods on recovery efficiency of manganese from manganese residue and harmless treatment. Chin J Environ Eng 11:6103–6108. https://doi.org/10.12030/j.cjee.201608105

Zhou C, Wang J, Wang N (2013) Treating electrolytic manganese residue with alkaline additives for stabilizing manganese and removing ammonia. Korean J Chem Eng 30:2037–2042. https://doi.org/10.1007/s11814-013-0159-8

Zhou L, Chen P, Hu C et al (2023) Study on the Mechanical Properties and Hydration Behavior of Steel Slag-Red Mud–Electrolytic Manganese Residue Based Composite Mortar. Appl Sci 13(10):5913. https://doi.org/10.3390/app13105913

Zulkifli M, Abu Hasan H, Sheikh Abdullah SR et al (2022) A review of ammonia removal using a biofilm-based reactor and its challenges. J Environ Manag 315:115162. https://doi.org/10.1016/j.jenvman.2022.115162

Authors and Affiliations

Zhihan Xie[1,2] · Rongjin Liu[1,2,3,4] · Fuhua Lu[1,2] · Daiyan Jing[2] · Yanrong Zhao[1,2,3,4] · Jianbo Liang[1,2] · Wanyu Huang[1,2] · Yuhang Liu[1,2]

✉ Rongjin Liu
liurj2008@sina.com

[1] College of Material Science and Engineering, Guilin University of Technology, Guilin 541004, China

[2] Collaborative Innovation Center for Exploration of Nonferrous Metal Deposits and Efficient Utilization of Resources in Guangxi, Guilin University of Technology, Guilin 541004, China

[3] Key Laboratory of New Processing Technology for Nonferrous Metal & Materials, Ministry of Education, Guilin University of Technology, Guilin 541004, China

[4] Guangxi Engineering and Technology Center for Utilization of Industrial Waste Residue in Building Materials, Guilin 541004, China